Materials Research Bulletin 44 (2009) 1743–1746

Contents lists available at ScienceDirect

Materials Research Bulletin

journal homepage: www.elsevier.com/locate/matresbu

Direct observation of the intergrown α-phase in β-$TmAlB_4$ via high-resolution electron microscopy

Kunio Yubuta [a,*], Takao Mori [b], Andreas Leithe-Jasper [c], Yuri Grin [c], Shigeru Okada [d], Toetsu Shishido [a]

[a] Institute for Materials Research, Tohoku University, Katahira 2-1-1, Aoba-ku, Sendai 980-8577, Japan
[b] International Center for Materials Nanoarchitectonics (MANA), National Institute for Materials Science (NIMS), Tsukuba 305-0044, Japan
[c] Max-Plank-Institut für Chemische Physik fester Stöffe, 01187 Dresden, Germany
[d] Department of Science and Engineering, Kokushikan University, Tokyo 154-8515, Japan

ARTICLE INFO

Article history:
Received 16 February 2009
Accepted 26 March 2009
Available online 5 April 2009

Keyword:
A. Inorganic compounds
C. Electron diffraction
C. Electron microscopy
D. Crystal structure

ABSTRACT

A $TmAlB_4$ crystal with a $ThMoB_4$-type (β-type) structure phase related to a hexagonal AlB_2-type structure was studied by electron diffraction and high-resolution electron microscopy. A high-resolution image clearly exhibits an intergrown lamellar structure of a $YCrB_4$-type (α-type) phase in the matrix of the β-type phase in $TmAlB_4$ crystal. The lamellar structure can be characterized by a tiling of deformed hexagons, which are a common structure unit in the α-type and β-type structures. The intergrown nanostructure is considered to be attributed to the origin of low temperature anomalies in physical properties.

© 2009 Elsevier Ltd. All rights reserved.

1. Introduction

The rare-earth metal borides have yielded intriguing systems to study fundamental problems in physics and chemistry [1]. The rare-earth metal aluminoboride system $RAlB_4$ has been attracting increasing attention with recent discoveries. Crystals with two different structure types were reportedly obtained from the same flux for $YbAlB_4$ and $LuAlB_4$ [2] with heavy fermion superconductivity observed for $YbAlB_4$ [3], while multiple magnetic transitions were reported to occur in $TmAlB_4$ at low temperatures below an antiferromagnetic transition temperature T_N [4]. $TmAlB_4$ takes a well-known $YCrB_4$-type structure [5] (space group *Pbam*), and we have found that X-ray diffraction measurements point to an intrinsic tiling variation existing in the crystals [6] due to the presence of fragments of the closely related $ThMoB_4$-type structure (space group *Cmmm*) [7]. Both structures have similarities to the AlB_2-type structure, with a planar boron network build of pentagonal and heptagonal rings having differently sized rare-earth and aluminum atoms. The difference between the $YCrB_4$-type (α-type) and $ThMoB_4$-type (β-type) structures is in the orientation of the pairs of condensed pentagonal rings. The lattice parameters for α- and β-type phases are $a = 0.59225$ nm, $b = 1.14784(5)$ nm and $c = 0.35224(2)$ nm, and $a = 0.72795(6)$ nm, $b = 0.93248(8)$ nm, and $c = 0.37981(3)$ nm, respectively. The previous work indicates that the existence of an intrinsic intergrown nanostructure influences physical properties and is the origin of multiple magnetic anomalies which are observed in $TmAlB_4$. This is striking because there are more than 100 compounds reported with this type of structure, and it is possible that such indicated phenomenon of the intrinsic tiling variation is actually ubiquitous.

With this interest in mind, we have attempted to observe directly the crystal structures of a successfully synthesized β-type $TmAlB_4$ crystal by high-resolution electron microscopy (HREM) to find a direct proof of the existence of such tiling variations.

2. Experimental

Samples were prepared via a two-step synthesis. First, a TmB_4 master alloy was made by reactive sintering (48 h at 1673 K) of compacted stoichiometric mixtures of thulium (Ames, 99.9 wt.%) filings and boron powder (crystalline, Chempur, 99.999 wt.%). All experimental steps were carried out inside an argon glove-box system (partial pressures of O_2 and $H_2O < 0.1$ ppm). In the second step, the binary tetraboride was powdered and compacted in a ratio of Tm:Al:B = 1:2:5 with aluminum filings (Chempur, 99.999 wt.%), placed in alumina crucibles, welded in Ta ampoules which were sealed in evacuated silica tubes. The tubes were then slowly heated to 973 K, kept there for 1 week, followed by regrinding and an additional heat treatment at 973 K for 2 weeks. Single phase polycrystalline samples were obtained. Magnetic

* Corresponding author. Tel.: +81 22 215 2199; fax: +81 22 215 2137.
E-mail address: yubuta@imr.tohoku.ac.jp (K. Yubuta).

0025-5408/$ – see front matter © 2009 Elsevier Ltd. All rights reserved.
doi:10.1016/j.materresbull.2009.03.013

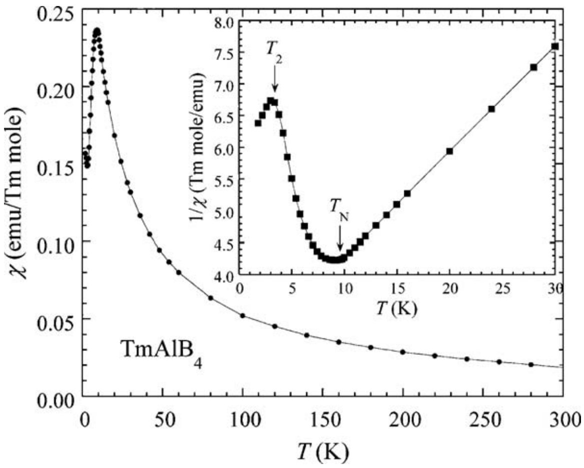

Fig. 1. Temperature dependence of the magnetic susceptibility χ of β-type $TmAlB_4$. The inset is an enlarged view of the inverse susceptibility at low temperatures.

susceptibility was measured using a Quantum Design MPMS-XL. Thin specimens for transmission electron microscopy (TEM) were prepared by dispersing crushed materials on holey carbon films. Electron diffraction (ED) patterns and HREM images were obtained using a 200 kV electron microscope (JEM-2010) at a resolution of 0.19 nm.

3. Results and discussion

The magnetic properties of β-type $TmAlB_4$ were investigated. The magnetic susceptibility χ (Fig. 1) exhibits a clear peak indicative of an antiferromagnetic transition at T_N = 9.5 K. As can be seen in the inset which shows an enlarged view of the inverse susceptibility, a further change of behaviour is observed below the Néel temperature at around T_2 = 3.5 K. Therefore, an anomaly below the Néel temperature is observed in β-type $TmAlB_4$ similar to that observed for α-type $TmAlB_4$ [6]. The Curie–Weiss fit of the χ data of β-type $TmAlB_4$ yields parameters of an effective magnetic moment $\mu_{eff} = 7.1\mu_B$/Tm and a Curie–Weiss temperature $\theta = -17$ K. The value of μ_{eff} is close to the theoretical value for the $^3H_6$ multiplet of the free trivalent thulium ion ($7.56\mu_B$).

Fig. 2(a) shows an ED pattern of the $TmAlB_4$ crystal, taken with the incident electron beam parallel to the [0 0 1] direction. Almost all of diffraction spots are those of the β-type phase.

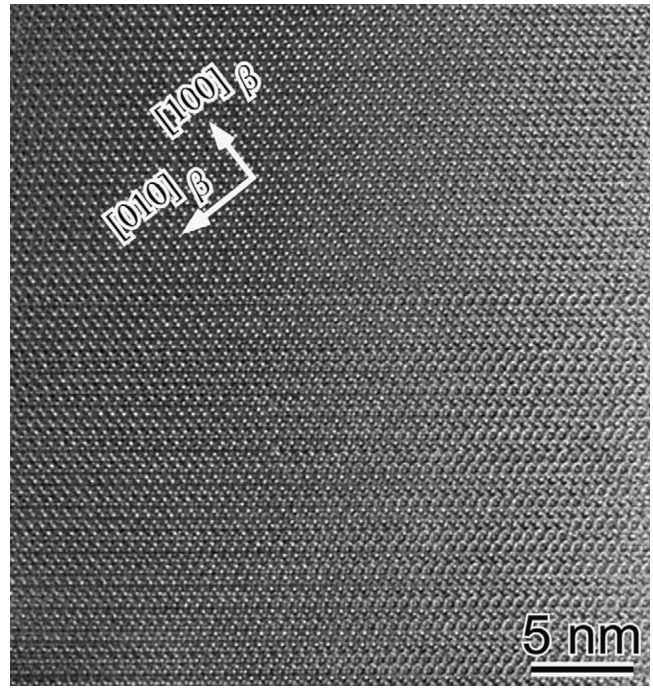

Fig. 3. A many-beam bright-field TEM image taken with the incident electron beam parallel to the [0 0 1] direction.

However, characteristic diffuse streaks, which suggest the existence of structural modulations, are observed along two directions d_1^* and d_2^*, indicated by large arrows in Fig. 2(a). Four white arrows in Fig. 2(a) correspond to reflection positions of the α-type phase, as shown in Fig. 2(b), which was taken from a α-type $TmAlB_4$ single crystal synthesized by the flux method [6,8]. Similar intensity distributions of strong Bragg reflections in the ED patterns, as indicated by arrowheads in Fig. 2(a) and (b), result from the fact that the structures of both phases are built by a unique structural unit, which consists of six heptagonal atomic columns containing edge-shared two pentagons (Fig. 5(a)).

Fig. 3 shows a HREM image taken with the incident beam of the same direction as Fig. 2(a). On the top part of Fig. 3, homogeneous lattice fringes of the β-type structure can be seen, whereas on the bottom part, a stacking modulation along the vertical direction is

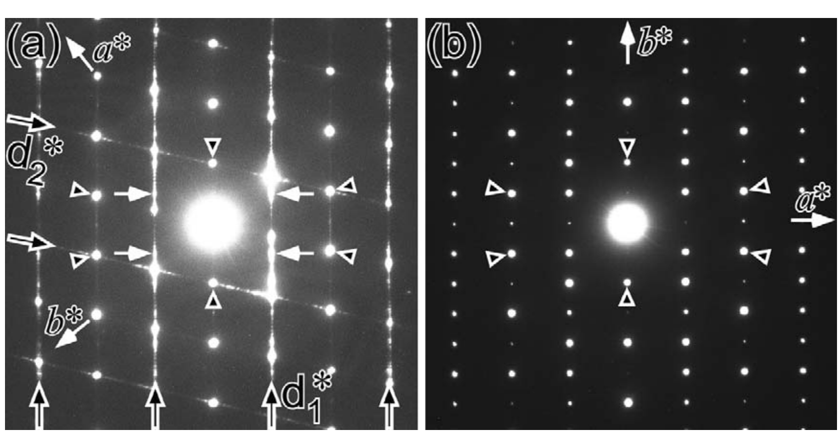

Fig. 2. ED patterns of (a) β- and (b) α-type phases taken with the incident electron beam parallel to the [0 0 1] direction. White arrows in (a) indicate reflection positions of the α-type phases. Large arrows in (a) indicate characteristic diffuse streaks. The α- and β-type phases belong to orthorhombic systems, space groups *Pbam* and *Cmmm*, respectively.

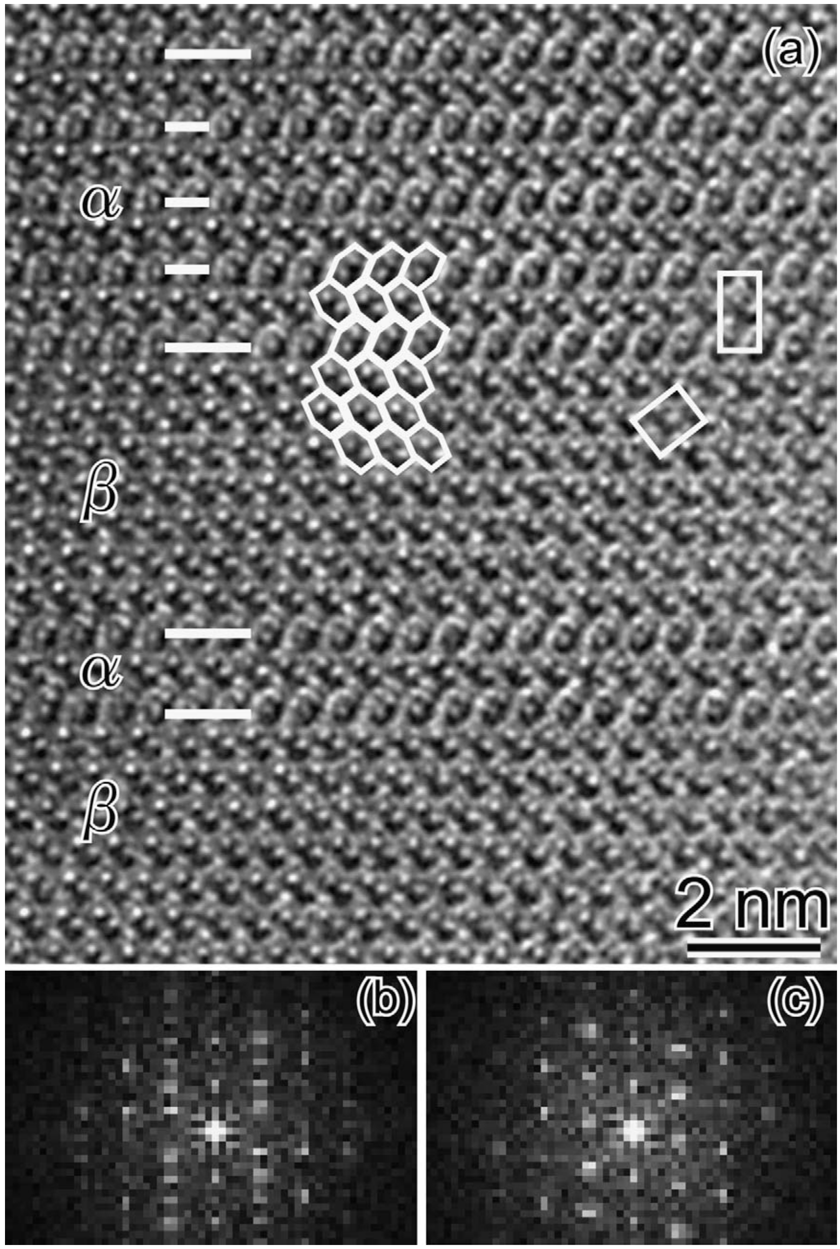

Fig. 4. An enlarged HREM image from a part of the intergrowth nanostructure. Deformed hexagons in (a) correspond to the structural unit in Fig. 5(a). The upper and lower rectangles in (a) indicate unit cells of the α- and β-type structures, respectively. Power spectra in (b) and (c) were obtained from regions of α- and β-type phases, respectively.

observed. In an enlarged HREM image of Fig. 4(a), one can see that the stacking modulation results from the local appearance of the α-type phase, viz., the intergrowth of the α-type phase in the β-type phase. The intergrowth structure may cause the low temperature anomalies in the physical properties. The upper and lower rectangles in Fig. 4(a) indicate unit cells of the α- and β-type phases, respectively. As shown by a tiling of deformed hexagons in the figure, the β-type phase can be characterized by a tiling of hexagons with one direction, whereas the α-type phase has a zigzag stacking of hexagons with two directions. The width of the lamella α-type phase along the *b*-axis is smaller than five unit cells. Fig. 4(b) and 4(c) show power spectra obtained from regions of the α- and β-type phases, respectively. The intensity distribution of the observed ED pattern of Fig. 2(a) can be easily understood by overlapping of those of Fig. 4(b) and 4(c). From the ED pattern and HREM image, it is confirmed that a crystallographic relationship between the β- and the α-type phases can be expressed as $(1\,\bar{1}\,0)_{\beta} \parallel (0\,1\,0)_{\alpha}$ and $[0\,0\,1]_{\beta} \parallel [0\,0\,1]_{\alpha}$.

Fig. 5 shows a structure model of the intergrowth of the α-type phase in the β-type phase. The both structures have a common hexagonal structural unit formed by connecting Tm atoms, as shown in Fig. 5(a). As can be seen from a tiling showing the intergrowth of the α-phase in the β-type matrix in Fig. 5(b), there are coherent interfaces parallel to the d_1 direction. The diffuse streaks along the direction d_1^* in Fig. 2(a) corresponds to the perpendicular direction of the interfaces parallel to the direction d_1. It is reasonable to consider that the diffuse streaks along the direction d_2^* originate from the twin-related micro-domains of the β-type phase, because the direction d_2^* is symmetrically equivalent to that of d_1^*.

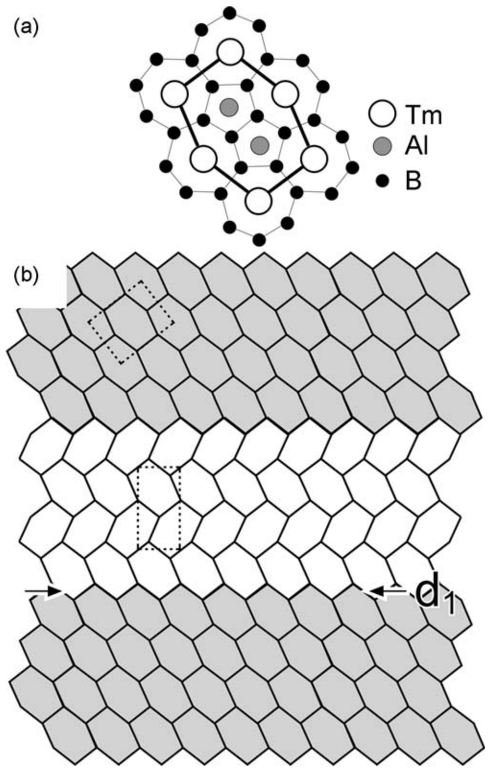

Fig. 5. (a) Structural unit of the deformed hexagon consisting of edge-shared two pentagonal and six heptagonal atomic columns. (b) Schematic illustration of a tiling of the deformed hexagons in the structure of an intergrowth α-phase in the β-type phases. The direction of arrows with letters d_1 is perpendicular to the d_1^* direction in the observed ED pattern of Fig. 2(a). Shade and open regions show the β- and α-type phases, respectively. Rectangles with dotted lines indicate unit cells of both phases.

4. Conclusions

In this report we have unequivocally demonstrated/proved the existence of an intergrowth nanostructure of the α-type phase in the β-type matrix. Through TEM observations, slivers of the α-type "tiling" were clearly observed to be insinuated into the β-type $TmAlB_4$ structure. The crystallographic relationship between the β- and the α-type phases can be expressed as $(1\,\bar{1}\,0)_\beta \parallel (0\,1\,0)_\alpha$ and $[0\,0\,1]_\beta \parallel [0\,0\,1]_\alpha$. We have also observed an antiferromagnetic transition at T_N = 9.5 K in β-type $TmAlB_4$ with a further low temperature anomaly below the Néel temperature at 3.5 K. This result agrees with our direct observation of the intergrowth structure and the hypothesis that the intergrowth is the origin of low temperature anomalies in the physical properties.

It still remains an interesting question of just how ubiquitous this phenomenon of the intergrown nanostructure is among such "tiled" compounds other than just $TmAlB_4$. Interesting behaviour has also been found in other β-type compounds such as the heavy fermion superconductivity recently discovered in $YbAlB_4$ [3] and it should be further investigated whether such intergrown nanostructure exists and might be playing any role in the physical properties of the Yb system also.

Acknowledgement

This study was partly supported by a Grant-in-Aid for Scientific Research from the Ministry of Education, Culture, Sports, Science and Technology of Japan.

References

[1] T. Mori, in: K.A. Gschneidner, Jr., J.-C. Bunzli, V. Pecharsky (Eds.), Higher Borides, Handbook on the Physics and Chemistry of Rare Earths, Vol. 38, North-Holland, Amsterdam, 2008, pp. 105–173.
[2] R.T. Macaluso, S. Nakatsuji, K. Kuga, E.L. Thomas, Y. Machida, Y. Maeno, Z. Fisk, J.Y. Chan, Chem. Mater. 19 (2007) 1918–1922.
[3] S. Nakatsuji, K. Kuga, Y. Machida, T. Tayama, T. Sakakibara, Y. Karaki, H. Ishimoto, S. Yonezawa, Y. Maeno, E. Pearson, G.G. Lonzarich, L. Balicas, H. Lee, Z. Fisk, Nature Phys. 4 (2008) 603–607.
[4] T. Mori, S. Okada, K. Kudou, J. Appl. Phys. 97 (2005), 10A910(1)–10A910(3).
[5] Y. Kuz'ma, Sov. Phys. Crystallogr. 15 (1970) 312–314.
[6] T. Mori, H. Borrmann, S. Okada, K. Kudou, A. Leithe-Jasper, U. Burkhardt, Yu. Grin, Phys. Rev. B 76 (2007), 064404(1)–064404(10).
[7] P. Rogl, H. Nowotny, Monatsh. Chem. 105 (1974) 1082–1098.
[8] S. Okada, K. Kudou, Y. Yu, T. Lundström, Jpn. J. Appl. Phys. 33 (1994) 2663–2666.